JOURNAL OF COMPUTATIONAL PHYSICS 7, 273–288 (1971)

Integration of the Planetary Vorticity Equation on a Parabolic Circular Grid

R. C. BEARDSLEY

Department of Meteorology, Massachusetts Institute of Technology, Cambridge, Massachusetts 02139

Received July 7, 1970

A nonuniform circular grid is defined based on equal azimuthal spacing and parabolic radial spacing for increased spatial resolution near the boundary. A conservative numerical scheme is devised to integrate the barotropic nondivergent potential vorticity equation. Examination of the truncation errors associated with the Jacobian and Laplacian approximations and trial integrations using linearized Rossby waves as exact solutions both indicate the parabolic scheme predicts linear fields poorly in a small annular region near the basin's center. Improved integrations are obtained with a modified numerical scheme.

1. INTRODUCTION

A laboratory model has been recently introduced by Pedlosky and Greenspan [5] which utilizes the physical analogy between vortex stretching by topography and the creation of relative vorticity by the β-effect to model the large-scale ocean circulation. The apparatus itself consists of the rapidly rotating cylindrical basin with sloping bottom. The applied wind stress is simulated by a viscous stress set up by the slow rotation of the flat top relative to the rest of the basin. The model response to a steady stress has been thoroughly studied [2], while questions concerning the model response to transient stresses are currently being explored experimentally.

The laboratory model is cylindrical in shape, so, as an initial step in the development of a complementary numerical model, a numerical scheme must be devised to integrate the governing equations in a circular basin. To increase computational speed and improve the spatial resolution of viscous boundary layer phenomena which we know will occur, especially along the western boundary, the polar grid should utilize a nonuniform distribution of grid points in the radial direction with a higher density of grid points near the basin's boundary. This paper discusses one particular choice of grid net and associated numerical scheme. The scheme is

conservative in the usual sense but the extreme nonuniform distribution of grid points causes large errors to appear near the center of the polar grid which do *not* decrease with an increase in spatial resolution. This unusual difficulty may be partially removed by modification of the original numerical scheme; so test calculations have been made for comparison. The more complex dynamics of the laboratory model may be reasonably approximated by the governing vorticity equation for two-dimensional, nondivergent flow of an incompressible viscous fluid on a β-plane, this latter balance having been extensively studied in a rectangular basin by K. Bryan [3] and others. However, to simplify the comparison, we will consider here in detail only the linearized planetary vorticity equation which yields inviscid Rossby waves as solutions.

2. Formulation of Numerical Scheme

The simplest grid for a circular domain consists of a uniform spacing between grid points in both the azimuthal and radial direction. However, adequate resolution near the boundary then causes an undesirable condensation of points near the center where, in general, the resolution requirements are less critical. An alternative approach which overcomes the problem of condensation near the center utilizes a grid spacing which decreases as r increases. Let η be a new radial coordinate defined by $\eta = f(r)$. The governing equations may then be transformed into the (η, θ)-coordinate system and provided $d\eta/dr \geqslant r^{\gamma}$, where $\gamma > 0$, a polar grid based on equal increments of η will have improved spatial resolution near the boundary. We consider here the specific function $\eta = r^2$. The grid is then defined by the set of $I \times J$ points, with coordinates

$$\eta_i = r_i^2 = i\Delta\eta, \quad i = 0, 1, \ldots, I,$$

$$\theta_j = j\Delta\theta \qquad , \quad j = 0, 1, \ldots, J,$$

where $\Delta\eta = 1/I$ and $\Delta\theta = 2\pi/J$. This grid offers about twice the radial resolution near the boundary as does a linear grid ($\eta = r$) with an equal number of radial grid points. Since $d\eta \propto r\, dr$, the area contained between two adjacent rings of grid points is constant. Thus, as the meridians diverge from the origin, the radial separation between mesh points decreases rapidly. The ratio of the maximum radial grid interval (adjacent to the origin) to the minimum is about $2\sqrt{I}$.

As mentioned before, our principal purpose here is to test the accuracy of the numerical scheme based on the r^2 transformation. While several approaches may be taken, we choose to consider the simpler physical system in which no external stress is applied on the fluid and internal friction and inertia are negligible (formally

letting both Rossby and Ekman numbers go to zero). The flow then satisfies the linearized conservation of potential vorticity equation,

$$\frac{\partial \zeta}{\partial t} = +J(\psi, y), \qquad \zeta = \nabla^2 \psi, \tag{1}$$

where ζ is vorticity, ψ the streamfunction, and $Y = 2y$, corresponding to βy. The transformed Jacobian is

$$J(\psi, g) = +2\{(\psi_\theta g)_\eta - (\psi_\eta g)_\theta\}. \tag{2}$$

This simple form of the Jacobian (identical to the Cartesian form) allows the conservative difference schemes of Arakawa [1] to be used directly. The circular boundary is impermeable so $\psi = 0$ at $r = 1$. This model was chosen for the test integrations so that analytic initial conditions with a known solution could be prescribed. Thus all errors are removed except those due to the numerical approximations used.

The finite difference analog to (1) considered here is

$$\begin{aligned}
\frac{\zeta_{ij}^{n+1} - \zeta_{ij}^{n-1}}{2\Delta t} &= -\mathbb{J}_{ij}(\psi, Y) \\
&= -\frac{1}{2\pi\Delta\eta} \sum_{j=0}^{J} Y_{1j}^n(\psi_{1,j-1}^n - \psi_{1,j+1}^n), \qquad i = 0, \\
&= -\frac{1}{2\Delta\theta\Delta\eta}\{Y_{ij+1}^n(\psi_{i+1j+1}^n - \psi_{i-1j+1}^n) \\
&\quad - Y_{ij-1}^n(\psi_{i+1j-1}^n - \psi_{i-1j-1}^n) \\
&\quad - Y_{i+1j}^n(\psi_{i+1j+1}^n - \psi_{i+1j-1}^n) \\
&\quad + Y_{i-1j}^n(\psi_{i-1j+1}^n - \psi_{i-1j-1}^n)\}, \qquad i > 0,
\end{aligned} \tag{3}$$

where the time derivative is estimated by centered differences (the leap frog method) and for $i > 0$, $\mathbb{J}$ is Arakawa's second-order kinetic energy conserving approximation (corresponding to $\mathbb{J}^{+\times}$ in his notation). At the origin, the Jacobian is computed from the net flux of Y (or "planetary vorticity") into the polygon-shaped area defined by the first ring ($i = 1$) of grid points. This expression coupled with Arakawa's formula does conserve kinetic energy in the sense that the finite difference approximation for the area integral of $\psi(\partial\zeta/\partial t)$ vanishes.

The Poisson problem of inverting the Laplacian to determine the streamfunction may be solved directly since the Laplacian operator is separable in the (η, θ)-

coordinate system. The finite difference Laplacian, derived from the integrated flux form of ∇^2, has the form

$$\bar{\nabla}^2_{ij}\psi = \frac{2\Delta\theta}{\pi\,\Delta\eta}\sum_{j=0}^{J}(\psi_{1j} - \psi_0), \qquad i = 0$$

$$= A_{+i}\psi_{i+1j} + A_{-i}\psi_{i-1j} + B_i\psi_{ij} + \frac{1}{i\,\Delta\eta\,\Delta\theta^2}(\psi_{ij+1} + \psi_{ij-1} - 2\psi_{ij}), \qquad i > 0 \tag{4}$$

where

$$A_{\pm i} = \frac{\psi}{\Delta\eta}\left(i \pm \frac{1}{2}\right), \qquad B_i = -\frac{8i}{\Delta\eta}.$$

Both ζ and ψ are represented by Fourier series of the form

$$\psi_{ij} = \sum_{k=0}^{J/2}\{C_k(i)\cos k\theta_j + S_k(i)\sin k\theta_j\},$$

where J is assumed to be even.

The unknown coefficients C_k and S_k satisfy the radial recurrence relationship obtained from (4) by the orthogonality property of the Fourier components. Only the axi-symmetric component of ψ contributes to the vorticity at the origin; so the appropriate boundary conditions for the unknown coefficients are

$$C_0(0) - C_0(1) = -\frac{\Delta\eta\,\zeta_0}{4}, \qquad S_k(0) = 0,$$

$$C_k(0) = S_k(0) = 0, \qquad k > 0,$$

$$C_k(I) = S_k(I) = 0, \qquad k \geqslant 0.$$

The resulting inversion problem to find C_k, S_k is solved by the Gaussian elimination method [6] to give an exact solution for ψ.

3. Estimation of Truncation Error

This numerical scheme utilizing an extremely nonuniform grid displays an unusual inaccuracy near the origin. The truncation error associated with the finite difference Jacobian at the origin is

$$\mathbb{J}_0(\psi, g) = J(\psi, g) + (\nabla^2 g)_{i=0}\cdot\frac{\Delta\eta}{8} - \left[\sum_{j=0}^{J}\{(g\psi_\theta)_{\theta\theta} - 4g\psi_{\theta\theta\theta}\}_{1j}\right]\frac{\Delta\theta^3}{24\pi\,\Delta\eta} + \cdots$$

and off center is

$$\mathbb{J}_{ij}(\psi, g) = J(\psi, g) + \{g_\theta \psi_{\eta\eta\eta} - 3(g_\eta \psi_{\eta\theta})_\eta\}_{ij} \frac{\Delta\eta^2}{3}$$
$$+ \{-g_\eta \psi_{\theta\theta\theta} + 3(g_\theta \psi_{\eta\theta})_\theta\}_{ij} \frac{\Delta\theta^2}{3} + \ldots, \qquad i > 0.$$

(The derivation of these expressions is discussed in Appendix A.) For any given number of radial grid points I, the number of azimuthal grid points J may be increased to make the truncation error associated with the azimuthal differentiation negligible. At the center the truncation error is of first order in $\Delta\eta$, or second order in physical space. Off center ($i > 0$), the truncation error is of second order in $\Delta\eta$. The finite difference equations thus are formally consistent in that the truncation error goes to zero at a fixed point in physical space (where the derivatives do not vary), as Δt, $\Delta\eta$, and $\Delta\theta \to 0$.[1]

The Taylor series expansion used above to estimate the truncation error fails to converge when ψ varies linearly with r. This peculiarity may be shown by examining the first-error term for the case of g and ψ behaving as r or $\sqrt{\eta}$. Then

$$(g_\theta \psi_{\eta\eta\eta})_i \, \Delta\eta^2 \propto \left(\frac{\Delta\eta}{\eta_i}\right)^2 = \frac{1}{i^2}$$

which clearly does not go to zero as $I \to \infty$. The scheme's inability to handle linear fields can be illustrated best by considering the total truncation error associated with the simple test function $\psi = x$. This streamfunction, corresponding to a spatially uniform northward flow, crudely approximates the lowest Rossby modes near the center of the circle.

Substitution of $\psi = x$ into the finite difference Jacobian (3) yields for the total fractional truncation error ϵ,

$$\epsilon \equiv \frac{J(x, Y) - \mathbb{J}_{ij}(x, Y)}{J(x, Y)} = 1 - \frac{\sin \Delta\theta}{\Delta\theta}, \qquad i = 0,$$

$$= 1 - \left[\frac{\sin \Delta\theta}{\Delta\theta}\right] 2 \sin^2 \theta_j - \left[\frac{\sin 2\Delta\theta}{2\Delta\theta}\right] \cos 2\theta_j \{\sqrt{i}\,(\sqrt{i+1} - \sqrt{i-1})\}, \qquad i > 0.$$

Since $\Delta\theta$ is typically $\ll 1$, the truncation error at the center is clearly negligible. Off center, the truncation error may be approximated by

$$\epsilon \doteq -(g_i - 1) \cos 2\theta_j,$$

[1] We use here a relaxed definition of consistency in which the numerical solution converges towards the true solution as $\Delta t \to 0$ everywhere except in a small annular ring about the center which may be made arbitrarily small by increasing I.

where the function g_i is defined by

$$g_i = \sqrt{i}\,(\sqrt{i+1} - \sqrt{i-1}).$$

TABLE I

Magnitude of Total Fractional Truncation Error ϵ Associated with the Trial Streamfunction $\psi = x$ as a Function of Radial Position

i	ϵ
1	41.4%
2	3.5%
3	1.5%
4	.8%

The error is periodic in θ with its azimuthal average being zero. The magnitude of the error $| g_i - 1 |$ decreases rapidly with increasing i as shown in Table I. For at least this test streamfunction $\psi = x$, the finite difference approximations are quite accurate at the center and for larger radii. However, the truncation error is quite large at the first few radial grid points. This increased error near the origin is unusual in the sense that as the number of radial grid points I is increased, the truncation error at a fixed point in physical space decreases but the error at the i-th radial position remains constant, independent of the magnitude of I. Thus an increase in I simply shifts the region of greater error closer towards the origin.

4. Modified Numerical Scheme

The inaccuracy displayed by the original numerical scheme can be partially removed by modification of the Jacobian in a small annular region near the origin. The original scheme is used at the center ($i = 0$) and outer ($i \geqslant 5$) grid points where the truncation errors discussed in the previous section are reasonably small. At intermediate grid points (located in the annular region $1 \leqslant i \leqslant 4$, $0 \leqslant j \leqslant J$), the governing linear vorticity Eq. (1) is reduced to

$$\frac{\partial \zeta}{\partial t} = 2\,\frac{\partial \psi}{\partial x} = 2\left\{\cos\theta\,\frac{\partial \psi}{\partial r} - \frac{\sin\theta}{r}\,\frac{\partial \psi}{\partial \theta}\right\},$$

and a numerical analog constructed as before using centered difference approximations for the time and azimuthal derivatives. The radial derivative at $r_i = \sqrt{i\Delta\eta}$ is estimated here by the average value of the derivative computed using centered

differences at $(r_{i-1} + r_i)/2$ and $(r_i + r_{i+1})/2$.[2] The modified numerical scheme then consists of (3) except in the annular region $(1 \leqslant i \leqslant 4, 0 \leqslant j \leqslant J)$ where

$$\frac{\zeta_{ij}^{n+1} - \zeta_{ij}^{n-1}}{2\,\Delta t} = \left\{ \frac{\cos\theta_j}{\sqrt{\Delta\eta}\,(\sqrt{i+1} - \sqrt{i})} (\psi_{i+1j} + (b_i - 1)\,\psi_{ij} - b_i\psi_{i-1j}) \right.$$

$$\left. - \frac{\sin\theta_j}{\Delta\theta\,\sqrt{i}\,\Delta\eta} (\psi_{ij+1} - \psi_{ij-1}) \right. ,$$

with

$$b_i \equiv \frac{\sqrt{i+1} - \sqrt{i}}{\sqrt{i} - \sqrt{i-1}} .$$

The truncation error associated with this modification is again formally of first order in $\Delta\eta$ and second order in $\Delta\theta$. However, the truncation error is now smaller, especially for nearly linear fields as demonstrated by the very small error $O(\Delta\theta^2)$ for the sample streamfunction $\psi = x$. The modified scheme no longer conserves kinetic energy but does predict $\partial\zeta/\partial t$ more accurately near the origin.

5. Analytic Test Fields

The linearized inviscid physical model was chosen for this study since it has well-known Rossby wave solutions (see [4] for complete description). Each mode consists of a vortical wave which travels to the west with a phase speed determined by the structure of the mode. We chose here to use as our analytic test solution the lowest mode with

$$\psi = J_0(k_1 r)\cos(k_1 r\cos\theta + \omega t), \tag{5}$$

where $\omega = 1/k_1$, k_1 being the first zero of the J_0 Bessel function. This mode consists of a simple plane wave with north-south phase lines traveling toward the west with phase speed $|\,C_p\,| = 1/k_1^2$ modulated by a stationary axi-symmetric envelope given by J_0.

6. Computed Truncation Error of Original Numerical Scheme

To test the error analysis presented in Section 3, the finite-difference Jacobian was evaluated using the analytic streamfunction (5) and compared with analytic values of $\partial\zeta/\partial t$ for two different relative phases of the mode. When the flow is

[2] This approximation for $\partial\psi/\partial r$ evaluated at r_i is equivalent to the usual centered difference formula which uses the known value of ψ at $r_{i+1} = r_i + \Delta r_i$ and the interpolated value of ψ at $r = r_i - \Delta r_i$. A second order approximation for the first derivative on a grid with unequal spacing does exist [7] but was unfortunately not used here.

TABLE II

Percent Magnitude of Maximum Error in $\partial\zeta/\partial t$ Prediction as Function of Radius r for Phases $t = 0$ and $t = \pi/2\omega$[a]

	$t = 0$		$t = \pi/2\omega$	
	L.R.	H.R.	L.R.	H.R.
0	0	0	10.6%	5.5%
.158	—	8.3%	—	+50.3
.224	9.3%	1.9	+64.6	+5.3
.275	—	.9	—	+3.0
.316	2.6	.6	+11.7	+2.6
.354	—	.5	—	+3.1
.387	1.5	.4	+16.0	+5.1

[a] Values based on calculations made with a low resolution (L.R.) grid (21 radial points) and a high resolution (H.R.) grid (41 radial points).

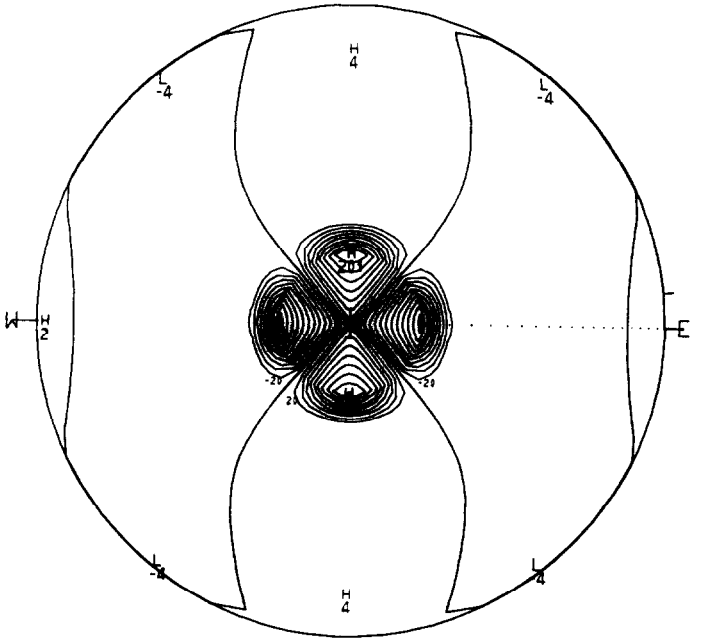

FIG. 1. Truncation error in Jacobian, i.e., $(\partial\zeta/\partial t)_{\text{analytic}} - \mathbb{J}$, at $t = \pi/2\omega$ for low resolution case ($I = 21$).

TABLE III

Percent Error $(\psi_a - \nabla^{-2}\zeta_a)/\psi_a$ in Vorticity Inversion Scheme as Function of Radius, Relative Phase of Field, and Spatial Resolution in Radial Direction

	$t = 0$		$t = \pi/2\omega$		$\sigma_\psi/\|\psi\|$ [a]	
r	L.R.	H.R.	L.R.	H.R.	L.R.	H.R.
.0	−1.7%	−0.5%	0	0	1.3%	0.4%
.158	—	−.3	—	11.4	—	3.2
.224	−1.1	−.2	11.9	6.3	4.7	2.5
.275	—	−.2	—	4.4	—	2.0
.316	−1.0	−.2	6.7	3.5	3.5	1.8
.354	—	−.2	—	2.9	—	1.6
.387	−1.0	−.2	4.9	2.5	3.0	1.5

[a] Last two columns list normalized standard deviation.

approximately circular about the center (corresponding to $t = 0$ in [5]), $\partial\zeta/\partial t = 0$ at the origin and $\mathbb{J}$ underestimates the Jacobian everywhere. The error contours are cloverleaf in shape with the maximum error occurring at the grid points nearest the origin along diagonals oriented at $\pm 45°$ to the x axis. An increase in radial resolution does shift the error towards the center as shown in Table II. One quarter-wave period later (corresponding to $t = \pi/2w$ in [5]), the flow consists of two vortical cells with essentially uniform motion in the $-y$ direction near the origin. Prediction of $\partial\zeta/\partial t$ by $\mathbb{J}$ is quite poor now with large over-and under-estimation occurring along the x and y axis near the origin. Figure 1 shows that the difference pattern $(\partial\zeta/\partial t)_{\text{analytic}} - \mathbb{J}$ does behave approximately like $\cos(2\theta)$ in the azimuthal direction as suggested earlier. While the magnitude of the difference decreases rapidly with increasing radius, the fractional error listed in Table II shows first this decrease and then a slight increase in the region where $\partial\zeta/\partial t = 0$. Again the error pattern shifts towards the center as $\Delta\eta$ is decreased.

The truncation error associated with the ∇^2 operator was also studied by comparing the analytic ψ with the numerical field obtained by inverting the analytic ζ corresponding to (5). The inversion scheme is quite accurate for $t = 0$ when the flow is roughly circular about the origin. This is to be expected since then both ψ and ζ vary spatially like r^2 near the origin. The truncation error is accordingly small for fields which are linear in η space. A quarter-wave period later ($t = \pi/2\omega$), both ψ and ζ behave like r or $\sqrt{\eta}$ near the center causing the inversion scheme to seriously underestimate ψ. The error pattern consists of two cells like ψ in shape with the maximum error concentrated along the x axis near the origin. Table III shows that the percentage error at the first few off-center grid points remains

relatively constant at $t = \pi/2\omega$ as the spatial resolution in η is increased. The average accuracy of the inversion scheme was estimated by computing the standard deviation of $(\psi_{\text{analytic}} - \psi_{\text{numerical}})$ over one wave period. Also listed in Table III, the standard deviation has been normalized by the envelope of ψ, $J_0(k_1 r)$, and reaches a maximum of 4.7 % at the first off-center grid point for the low resolution case.

TABLE IV

Error in Phase Speed Observed in Four Test Integrations[a]

	Original Scheme	Modified Scheme
$I = 21$	2.1 %	2.2 %
$I = 41$	1.4 %	1.4 %

[a] For all integrations, the number of azimuthal grid points was constant, $J = 56$, and the time step $\Delta t = 0.005T$ where T is the period of the lowest Rossby mode.

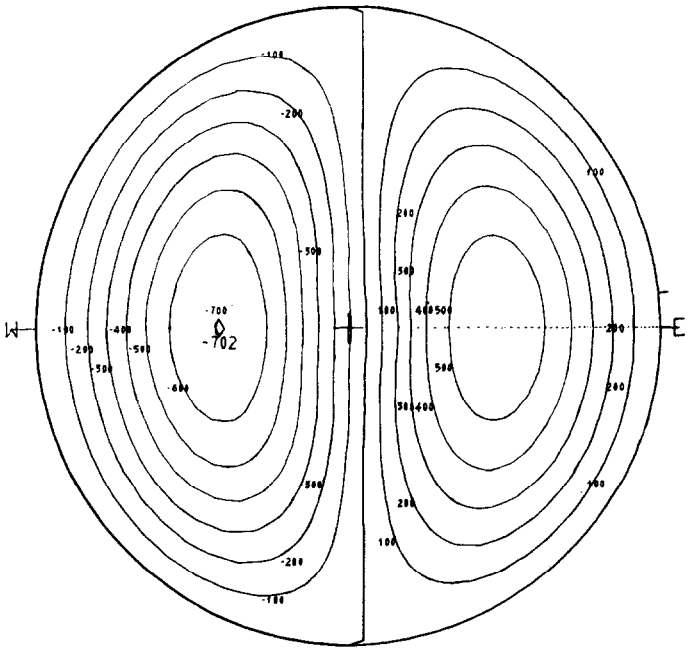

FIG. 2. ψ predicted by original scheme at $t = 3\pi/\omega$ for high resolution case ($I = 41$).

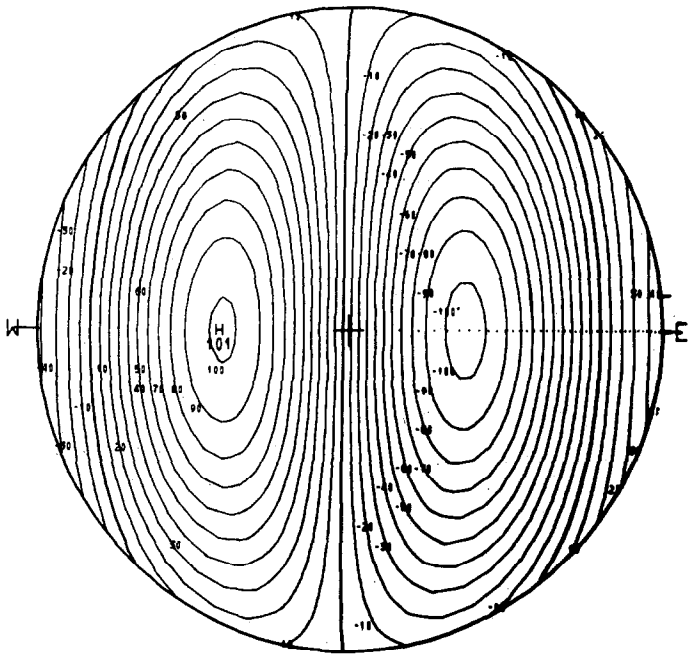

FIG. 3. (a) Analytic ζ. Vorticity prediction at $t = 3\pi/\omega$ for high resolution case ($I = 41$).

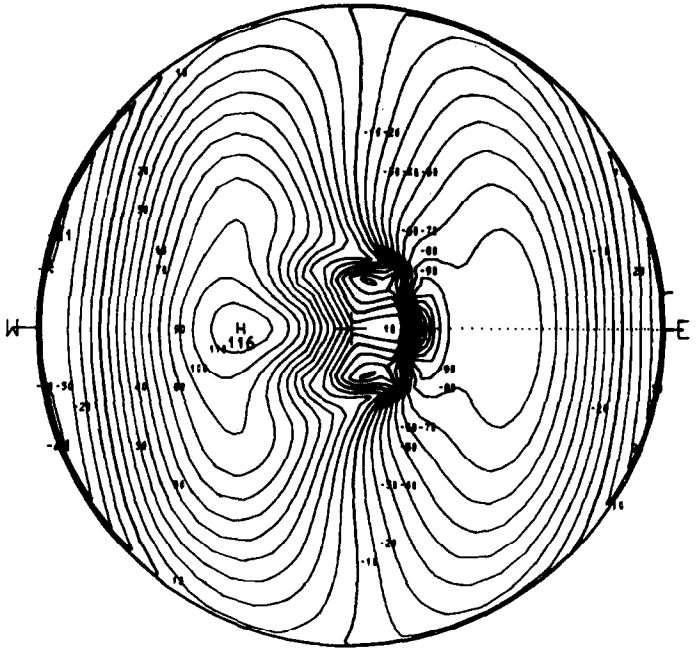

(b) ζ predicted by original numerical scheme.

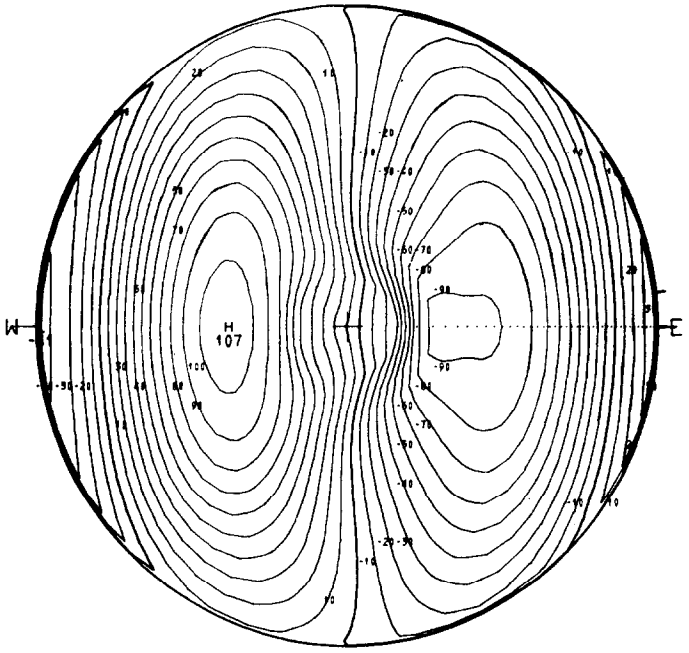

(c) ζ predicted by modified numerical scheme.

7. Two and Four Period Integrations

The large truncation error exhibited by both operators practically rules out use of the r^2 grid for numerical calculations in a circular basin. We will proceed with the test integrations to see how the Rossby wave mode is distorted by the scheme with time. Both the original and modified numerical schemes were integrated from initial ζ and ψ fields (corresponding to [5] at $t = 0$ and $t = \Delta t$) for a total duration of two periods over a grid with 41 radial grid points and four periods over a grid with 21 grid points. The time step ($t = 0.1\,\pi/\omega$) was chosen to keep the estimated time differencing error less than 0.1 % for the worst case. The numerical solutions at even and odd time steps were consistent and did not noticeably diverge.

In all cases, the Rossby mode moved to the west with the streamfunction exhibiting relatively little variation from the analytic field. Figure 2 shows ψ at $t = 3\pi/\omega$ for the original scheme. The modified prediction appears identical. Both fields show a slight deviation from the analytic field in the bending of streamlines near the origin and phase lag. The observed westward phase speed is only slightly smaller than the theoretical value with a maximum difference of 2.2 % (see Table IV

for phase speed comparison and listing of integration parameters). The original scheme does conserve kinetic energy while the modified scheme shows a small periodic variation in kinetic energy due primarily to truncation error.

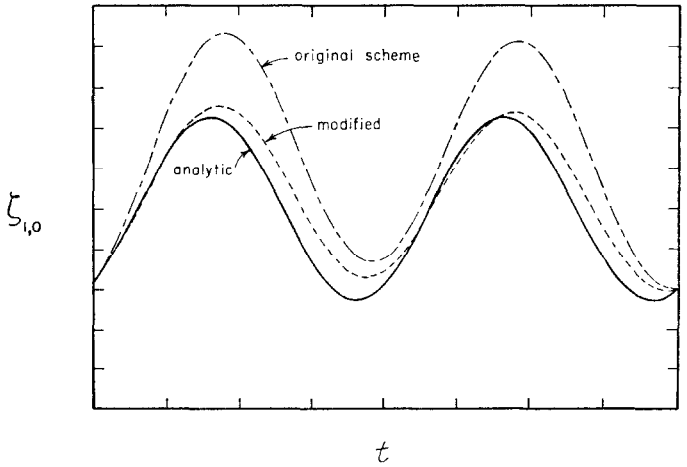

FIG. 4. ζ predicted by original and modified schemes for high resolution case ($I = 41$) at the first off-center grid point along x axis ($i = 1, j = 0$).

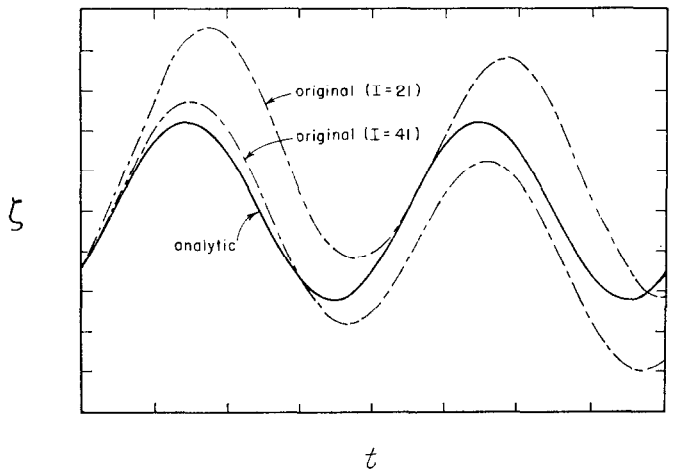

FIG. 5. ζ predicted at some off-center point on x axis using original scheme with different radial resolution. Point corresponds to $i = 1$ for low resolution case ($I = 21$) and $i = 2$ for high resolution case ($I = 41$).

The predicted vorticity field at $t = 3\pi/\omega$ (shown in Fig. 3) clearly indicates marked deviation from the analytic field. While the original scheme accurately predicts ζ near the circular boundary, the predicted field is quite contorted near the origin, principally around the first few rings of grid points. Since some part of the apparent distortion very close to the origin may be due to the computer contouring and plotting routine, the fields should be examined at points in physical space corresponding to mesh points for different grid resolution cases. The maximum deviation in ζ characteristically occurs at the first off-center ring of grid points. Figure 4 compares ζ predicted by original and modified schemes (for the high resolution case) at the first off-center point along the x axis. Both schemes tend to overestimate ζ (the original scheme by $\sim 100\,\%$ at $t = \pi/\omega$), causing the time averaged vorticity to become positive. The next radial point away from the center along the x axis partially compensates by acquiring negative average vorticity. Since this point for the high resolution case coincides in physical space with the first off-center point in the low resolution case, the predictions for both cases are shown in Fig. 5. Initially at least, the high resolution ζ prediction is better. Note that the low resolution prediction at $i = 1$ is almost identical to ζ at the first grid point ($i = 1$) for the high resolution case (shown in Fig. 4). This again emphasizes that accuracy may be improved at a fixed point in space by decreasing $\Delta\eta$ but prediction at the first off-center grid points will remain uniformly poor.

8. Critique

A numerical scheme based on a r^2 grid has been devised to integrate the simple β-plane vorticity balance. The r^2 transformation was chosen for its simplification of the Jacobian and concentration of grid points near the boundary. A critical discussion of the truncation errors associated with the different numerical operators and the results of trial integrations both indicate that the scheme fails. Gross errors arise near the origin where, inherently limited by the r^2 transformation, the scheme cannot accurately handle linear fields. While both Jacobian and Laplacian operators give reasonable predictions for parabolic fields, the large error in $\partial\zeta/\partial t$ for linear fields causes large over- and under-shoot in ζ during the initial phase of the test integrations. The modified numerical scheme yields better results since it approximates $\partial\zeta/\partial t$ more accurately for linear fields. These large deviations occur in a physically small region near the center and approximately average to zero; so the Rossby waves making up the standing mode pass through the central region to emerge relatively undistorted. The predicted streamfunction shows little distortion anywhere since errors in the vorticity field are inherently smoothed in the inversion process.

APPENDIX A: CALCULATION OF TRUNCATION ERROR

The truncation error associated with the Jacobian approximation given in (3) may be calculated at the off-center grid points in the usual manner. The values of ψ and g at adjacent grid points are found by Taylor series expansions and substituted into $\mathbb{J}_{ij}$ to give the expression presented in Section 3.

This method must be slightly modified at the origin. The Jacobian when integrated over the area A defined by $0 \leqslant r \leqslant r_1 = \sqrt{\Delta\eta}$, $0 \leqslant \theta \leqslant 2\pi$, is equal by the divergence theorem to

$$\tfrac{1}{2} \iint_A J(\psi, g)\, d\eta\, d\theta = \int_0^{2\pi} (g\vec{Q} \cdot \hat{r})_{i=1}\, r_1\, d\theta, \tag{A-1}$$

where $\vec{Q} = \hat{k} \times \nabla\psi$ and $\hat{r}$ is a unit vector directed radially outward. Expansion of J about the origin before integration yields for the left side

$$\tfrac{1}{2} \iint_A J(\psi, g)\, d\eta\, d\theta = [J(\psi, g)_{i=0}]\, \pi\, \Delta\eta + [\nabla^2 J(\psi, g)_{i=0}] \frac{\pi\, \Delta\eta^2}{8} + \cdots.$$

The integrand of the contour integral may be further simplified using the stream-function definition before expansion and integration to give for the right side

$$\int_0^{2\pi} \left(g \frac{\partial\psi}{\partial\theta}\right)_{i=1} d\theta = \sum_{j=0}^{J} \int_{\theta_{j-1/2}}^{\theta_{j+1/2}} (g\psi_\theta)_{i=1}\, d\theta$$

$$= \sum_{j=0}^{J} \left\{(g\psi_\theta)_{i=1,j}\, \Delta\theta + ((g\psi_\theta)_{\theta\theta})_{i=1,j} \frac{\Delta\theta^3}{24} + \cdots\right\}.$$

Since

$$\psi_{\theta j} = \frac{\psi_{j+1} - \psi_{j-1}}{2\,\Delta\theta} - \frac{1}{6}\, \psi_{\theta\theta\theta j}\, \Delta\theta^2 + \cdots,$$

the contour integral becomes

$$\sum_{j=0}^{J} \left\{\left[\frac{g_j(\psi_{j+1} - \psi_{j-1})}{2}\right]_{i-1} + \left[\frac{(g\psi_\theta)_{\theta\theta} - 4g\psi_{\theta\theta\theta}}{24}\right]_{i-1,j} \Delta\theta^3 + \cdots\right\}.$$

The first sum may be identified as the area $\pi\Delta\eta$ times the finite difference expression given in (3) for J at the origin. The truncation error estimate given in Section 3 may then be obtained by equating both sides of A-1 and rearranging terms.

ACKNOWLEDGMENTS

I would like to thank Dr. D. L. Williamson for several helpful discussions at NCAR where most of the computations were made. I also appreciate the assistance of Mr. D. Robertson, who helped modify the contouring routines for the *dd*80 visual display unit at NCAR, and J. Festa of MIT who helped with the coding. This research represents M.I.T. G.F.D. Lab. Report No. 70-2 and was supported by the Office of Naval Research [contract Nonr-1841(74)]. Acknowledgment is also made to NCAR, which is sponsored by NSF, for use of its CDC 6600 computer.

REFERENCES

1. A. ARAKAWA, Computational design for long-term numerical integration of the equations of fluid motion: Two-dimensional incompressible flow, Part 1, *J. Computational Phys.* **1** (1966), 119–143.
2. R. C. BEARDSLEY, A laboratory model of the wind-driven ocean circulation, *J. Fluid Mech.* **38** (1969), 255–271.
3. K. BRYAN, A numerical investigation of a non-linear model of a wind driven ocean, *J. Atmos. Sci.* **20** (1963), 594–606.
4. H. P. GREENSPAN, "The Theory of Rotating Fluids," Cambridge Univ. Press, 1968.
5. J. PEDLOSKY AND H. P. GREENSPAN, A simple laboratory model for the ocean circulation, *J. Fluid Mech.* **27** (1967), 291–304.
6. R. RICHTMEYER AND R. MORTON, "Difference Methods for Initial Value Problems," Interscience, New York, 1967.
7. H. SUNDQVIST AND G. VERONIS, A simple finite-difference grid with non-constant intervals, *Tellus* **22** (1970), 26–31.